

**VOLUME CRYSTALLIZATION OF A NICKEL DROPLET  
CONTAINING REFRACTORY NANOPARTICLES  
UPON ITS IMPACT ONTO A SUBSTRATE**

**A. N. Cherepanov, V. N. Popov, and O. P. Solonenko**

UDC 532.501.32:669.14.018.28

*A mathematical model is developed for nonequilibrium volume crystallization of a metallic droplet modified by mechanically activated refractory nanoparticles upon its impact onto a solid substrate. The model takes into account the kinetics of heterogeneous and homogeneous nucleation during melt cooling. Specific features of crystallization of a liquid metal (nickel) depending on the concentration and size of modifying particles are examined numerically. A typical feature of the process considered is the maximum supercooling of the melt, whose magnitude depends on the particle size and cooling intensity. Homogeneous nucleation is almost absent. The calculated radii of droplets solidified on the substrate are in good agreement with available experimental data.*

**Key words:** droplet, substrate, modification, nanoparticles, crystallization, nucleation.

**Introduction.** Much attention has been paid recently to improving the quality of the surface of various articles and mechanisms. One promising method of solving this problem is plasma spraying, which ensures high-quality metallic and composite coatings [1, 2]. Important factors responsible for the set of physical, mechanical, and exploitation properties of such coatings are the internal interfaces between splats (solidified metallic droplets), the interfaces between splats and the substrate surface, and the internal structure of splats themselves. The basic functional parameters determining the properties of plasma coatings are the strength of their adhesion to the substrate surface, porosity, crystalline structure, and phase composition.

Preliminary experimental studies [3] on spraying mechanically activated metallic powders modified by ultrafine ceramic particles (nanoparticles) showed that the resultant coatings possess higher adhesion, higher density, and more uniform structural components, as compared to reference samples.

An experimental investigation and improvement of the processes of high-velocity interaction of droplets with the substrate is a complicated problem from both the methodical and technical viewpoints. Optimization of the technological process requires the knowledge of the whole variety of inherent phenomena: heat exchange with the substrate, droplet deformation, nucleation and growth of crystals, etc. Therefore, the most effective method of studying these processes is mathematical modeling.

A mathematical model of spreading and crystallization of a liquid metallic droplet modified by an ultrafine powdered refractory compound is considered below.

**Formulation of the Problem. Assumptions.** We consider the kinetics of solidification of a liquid metallic particle (droplet) after its impact onto a solid substrate. A particle of volume  $V_0$  is assumed to impact onto the substrate at a right angle with a certain velocity  $v$  and starts spreading on the substrate surface, retaining the shape of a spheroidal segment during its motion. The particle substance is a pure metal pre-modified by an ultrafine powder of a refractory compound. The mass content of the powder particles in the melt is low (less than 0.05%), and their size  $R_p$  is much smaller than the characteristic size of the liquid droplet; hence, the influence of the ultrafine

---

Institute of Theoretical and Applied Mechanics, Siberian Division, Russian Academy of Sciences, Novosibirsk 630090; ancher@itam.nsc.ru. Translated from *Prikladnaya Mekhanika i Tekhnicheskaya Fizika*, Vol. 47, No. 1, pp. 29–34, January–February, 2006. Original article submitted December 30, 2004; revision submitted April 29, 2005.

powder on the physical parameters of the liquid can be ignored. The powdered particles are mechanically activated and serve as active centers of crystallization. The temperature of the substrate and the ambient temperature are lower than the metal-crystallization temperature.

To simplify the problem, we use the following assumptions.

1. The characteristic size  $d$  of the liquid particle is rather small, and the substrate surface contains an oxide film; as a result, the internal thermal resistance of the particle is much lower than its external thermal resistance [ $d/\lambda \ll 1/\alpha$ , where  $\lambda$  is the thermal conductivity of the metal and  $\alpha = \lambda_3/\delta_3$  ( $\delta_3$  and  $\lambda_3$  are the thickness and thermal conductivity of the film)].
2. The substrate in the initial state is heated to a temperature below the melting point of its material and initial temperature of the droplet, whereas the droplet is overheated above the equilibrium melting point so that the absence of nucleation and growth of the solid crystalline phase at the stage of droplet spreading can be postulated.
3. The law of motion of the contact spot  $R_c$  is known and is described by the expression [4]

$$R_c(t) = 0.922R_0 \left( \frac{2R_0\nu}{\nu_1} \right)^{1/4} \left\{ 1 + \frac{1}{\pi} \left[ \sqrt{\frac{vt}{R_0} \left( 2 - \frac{vt}{R_0} \right)} - 2 \arctan \sqrt{\frac{2 - vt/R_0}{vt/R_0}} \right] \right\}, \quad (1)$$

where  $R_0$  is the initial droplet radius,  $\nu$  is the kinematic viscosity of the melt, and  $t$  is the time.

**Governing Equations and Boundary Conditions.** Under the assumptions made, we consider metal solidification as a volume process, and the temperature distribution during cooling and crystallization of the metal is assumed to be uniform. All ultrafine particles are assumed to be crystallization centers.

The cylindrical coordinate system  $z, r$  is chosen to have the origin at the center of the spheroidal segment; the  $r$  axis lies in the plane of the substrate surface and the  $z$  axis is directed downward to the substrate.

The equation of the heat balance in the solidifying droplet yields a differential equation for the volume-averaged particle temperature  $T_1$ :

$$M_1 c_1 \frac{dT_1}{dt} = F_c \lambda_2 \left. \frac{\partial T_2}{\partial z} \right|_{z=0} - F_f \alpha_f (T_1 - T_g) + M_1 \varkappa_1 \frac{df_s}{dt}, \quad f_s \equiv 1 \quad \text{at} \quad T < T_e. \quad (2)$$

The terms in the right side of this equation describe heat transfer to the substrate (first term), radiative heat transfer into the ambient medium (second term), and latent heat release during crystallization (third term);  $M_1$  is the particle mass,  $c_1$  is the heat capacity of the metal,  $T_2$  is the substrate temperature,  $F_c$  is the contact-spot area,  $\lambda_2$  is the thermal conductivity of the substrate,  $F_f$  is the area of the free surface of the droplet,  $\alpha_f = \varepsilon \sigma_0 (T_1^2 + T_g^2) (T_1 + T_g)$  is the coefficient of radiative heat transfer between the free surface of the particle and the ambient medium (gas),  $\varepsilon$  is the reduced emissivity,  $\sigma_0$  is the Stefan–Boltzmann constant,  $\varkappa_1$  is the crystallization heat,  $f_s$  is the cross section (fraction) of the solid phase,  $T_g$  is the temperature of the ambient gas, and  $T_e$  is the equilibrium crystallization temperature; the subscripts 1 and 2 refer to the droplet and substrate parameters, respectively.

The values of  $F_c(t)$  and  $F_f(t)$  are determined by the relations

$$F_c(t) = \pi R_c^2(t), \quad F_f = \pi (R_c^2 + H^2), \quad (3)$$

where  $H$  is the height of the solidifying particle obtained from the condition of a constant volume of the particle:

$$(4\pi/3)R_0^3 = (\pi/6)H(3R_c^2 + H^2).$$

Therefore, we obtain

$$H(t) = R_0 \left[ \sqrt[3]{\sqrt{(R_c/R_0)^6 + 16} + 4} - \sqrt[3]{\sqrt{(R_c/R_0)^6 + 16} - 4} \right]. \quad (4)$$

The substrate temperature  $T_2$  is determined by solving the heat-conduction equation for a cylindrical domain corresponding to the contact spot

$$c_2 \rho_2 \frac{\partial T_2}{\partial t} = \frac{\lambda_2}{r} \frac{\partial}{\partial r} \left( r \frac{\partial T_2}{\partial r} \right) + \lambda_2 \frac{\partial^2 T_2}{\partial z^2} \quad (5)$$

with the boundary conditions

$$T_2 \Big|_{t=0} = T_{20}, \quad \left. \frac{\partial T_2}{\partial r} \right|_{r=0} = 0, \quad \left. \frac{\partial T_2}{\partial r} \right|_{r=R_c} = 0; \quad (6)$$

$$\lambda_2 \left. \frac{\partial T_2}{\partial z} \right|_{z=0} = \alpha (T_2 \Big|_{z=0} - T_1), \quad \left. \frac{\partial T_2}{\partial z} \right|_{z=h_2} = 0, \quad (7)$$

where  $h_2$  is the substrate thickness and  $\alpha = \lambda_3/\delta_3$  is the coefficient of heat transfer from the droplet to the substrate. The subscript 3 is used to indicate the parameters of the oxide film. The third condition in (6) is the condition of adiabaticity on a cylindrical boundary whose radius coincides with the contact-spot radius. This assumption is valid for the problem considered because the Peclet number characterizing the ratio between the convective and conductive heat transfer is much greater than unity [ $\text{Pe} = v_c R_c / (\lambda_1 / c_1 \rho_1) \gg 1$ , where  $v_c$  is the characteristic velocity of the contact-spot boundary].

We supplement Eqs. (2)–(7) by a relation that describes the kinetics of solid-phase growth on nucleation centers (seeds), which are refractory ultrafine powder nanoparticles. We assume that a unit volume of the initial melt contains  $N_p$  seeds (nanoparticles) on which the crystalline phase starts growing. The growth rate of the crystals is described by the power law [5, 6]

$$v_k = K_v (T_e - T)^m, \quad (8)$$

where  $K_v$  is the growth-rate constant and  $m$  is an indicator characterizing the mechanism of crystal growth ( $m = 1$  and  $m = 2$  refer to the conventional and dislocation mechanisms, respectively). We assume that the seeds have a spherical shape. In this case, the growth of the solid phase follows the law [5, 8]

$$f_s = 1 - \exp \left\{ -\varphi \left[ N_p \left( R_p + K_v \int_{t_e}^t \Delta T^m d\xi \right)^3 + \int_{t_e}^t J_n(\xi) \left( K_v \int_{\xi}^t \Delta T^m d\zeta \right)^3 d\xi \right] \right\}, \quad (9)$$

where  $f_s$  is the fraction of the solid phase,  $\varphi = 4\pi/3$ ,  $N_p$  is the number of nanoparticles in a unit volume of the melt,  $t_e = t(T_e)$  is the time corresponding to the moment the melt is cooled down to the equilibrium crystallization temperature  $T_e$ ,  $\Delta T = T_e - T$  is the supercooling of the melt, and  $J_n(t)$  is the rate of homogeneous nucleation described by the formula [7]

$$J_n(t) = K_n \exp \{ -[U + W/(\Delta T)^2] \}, \quad (10)$$

where  $K_n = 2nd_m \sqrt{\sigma_1 kT}/h$ ,  $W = 16\pi\sigma_1^3 T_e^2 / [3(\varkappa\rho_1)^2 kT]$ ,  $n$  is the number of atoms in a unit volume of the melt,  $d_m$  is the atom diameter,  $\sigma_1$  is the surface tension, and  $h$  is the Planck constant.

Thus, the problem reduces to solving the system of integrodifferential equations (2), (5), and (9) with allowance for relations (1)–(4), (8), and (10) and boundary conditions (6) and (7). An algorithm based on the Runge–Kutta and finite-difference methods was used for numerical implementation of the resultant system.

The initial data for the nickel droplet [9] were  $R_0 = 10^{-5}$  m,  $v = 50$  m/sec,  $K_v = 0.025$  m/(sec·K),  $m = 1$ ,  $n_1 = 8.06 \cdot 10^{28}$  1/m<sup>3</sup>,  $T_{10} = 1828$  K,  $\rho_1 = 7.79 \cdot 10^3$  kg/m<sup>3</sup>,  $\lambda_1 = 71.5$  W/(m·K),  $c_1 = 735$  J/(kg·K),  $\nu_1 = 5.7 \cdot 10^{-7}$  m<sup>2</sup>/sec,  $\varkappa_1 = 3.056 \cdot 10^5$  J/kg,  $T_e = 1728$  K,  $T_g = 303$  K,  $\varepsilon = 0.35$ , and  $\sigma_0 = 5.67 \cdot 10^{-8}$  J/(m<sup>2</sup>·K); the initial data for the steel substrate were  $h_2 = 3 \cdot 10^{-3}$  m,  $T_{20} = 970$  K,  $\rho_2 = 7.25 \cdot 10^3$  kg/m<sup>3</sup>,  $\lambda_2 = 16.78$  W/(m·K),  $c_2 = 650$  J/(kg·K),  $\lambda_3 = 3.5$  W/(m·K), and  $\delta_3 = (5-10) \cdot 10^{-6}$  m.

**Analysis of Results.** Cooling and crystallization of the droplet after its impact onto a solid steel substrate (steel 1Kh18N9T) and subsequent spreading are analyzed numerically. As was noted above, to satisfy the condition of volume crystallization, it is necessary to ensure a moderate intensity of heat transfer from the droplet to the substrate, in order to have low temperature gradients inside the droplet during cooling and crystallization. This can be achieved by substrate heating, which is done in real spraying conditions; in this case,  $\text{Bi}_1 = \lambda_3 R_0 / (\lambda_1 \delta_3) \ll 1$ . It was assumed in calculations, therefore, that the substrate surface is coated by an oxide film of thickness  $\delta_3 \geq 5$   $\mu\text{m}$ . If the thermal conductivity of the film (e.g., FeO) is  $\lambda_3 = 3.5$  W/(m·K), the Biot number for a nickel droplet of radius  $R_0 = 10$   $\mu\text{m}$  with the thermal conductivity of the metal  $\lambda_1 = 71.5$  W/(m·K) is  $\text{Bi}_1 \leq 0.05$ . To satisfy this condition, the oxide-film thickness in calculations was assumed to be 5–10  $\mu\text{m}$ .

The influence of the size and concentration of modifying particles on the melt-crystallization kinetics was considered. The calculated results are plotted in Figs. 1–4, where  $\Delta\theta_1 = 1 - T_1/T_e$ ,  $\theta_1 = T_1/T_e$ , and  $\tau = at/R_0^2$ . As is seen from the position of the cooling curve (Fig. 1), its typical feature is the existence of the maximum supercooling of the melt  $\Delta\theta_{1\text{max}}$ , which is reached at the beginning of the crystallization process, and the minimum supercooling  $\Delta\theta_{1\text{min}}$ , which remains almost unchanged up to the end of the process. The transition from  $\Delta\theta_{1\text{max}}$  to  $\Delta\theta_{1\text{min}}$  is caused by intensified growth of the solid phase. This leads to heating (recalescence) of the supercooled melt owing to release of crystallization heat.

As the particle diameter is reduced, the maximum supercooling and the recalescence time also decrease. For instance, the maximum supercooling is  $\Delta T_{\text{max}} = 12.1$  K for  $\delta_3 = 5$   $\mu\text{m}$  and  $R_p = 2.5 \cdot 10^{-8}$  m and  $\Delta T_{\text{max}} = 19$  K for

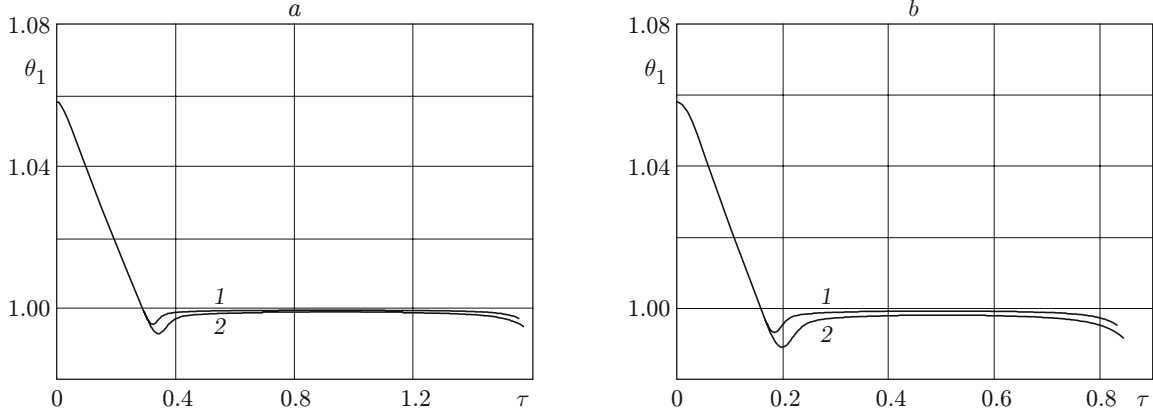


Fig. 1. Temperature of the droplet of the modified melt during its volume crystallization on a substrate for different values of the oxide-film thickness  $\delta_3$  and nanoparticle radius  $R_p$ : (a)  $\delta_3 = 10 \mu\text{m}$  and  $R_p = 0.025$  (1) and  $0.05 \mu\text{m}$  (2); (b)  $\delta_3 = 5 \mu\text{m}$  and  $R_p = 0.025$  (1) and  $0.05 \mu\text{m}$  (2).

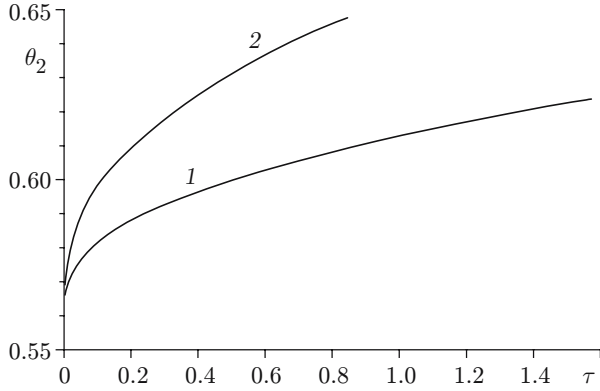


Fig. 2

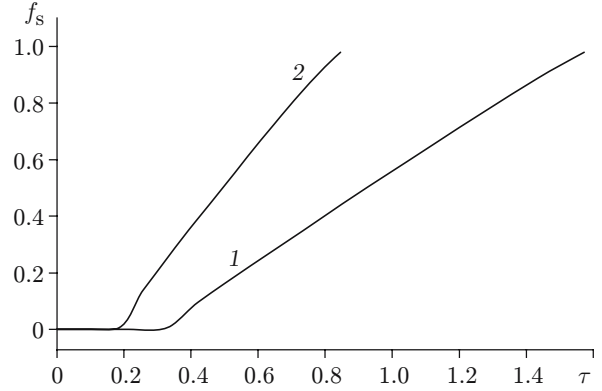


Fig. 3

Fig. 2. Temperature of the substrate surface in the contact region during droplet cooling for  $\delta_3 = 10$  (1) and  $5 \mu\text{m}$  (2);  $R_p = 0.025\text{--}0.05 \mu\text{m}$ .

Fig. 3. Kinetics of growth of the volume fraction of the solid phase during droplet crystallization on the substrate for  $\delta_3 = 10$  (1) and  $5 \mu\text{m}$  (2);  $R_p = 0.025\text{--}0.05 \mu\text{m}$ .

$R_p = 5 \cdot 10^{-8} \text{ m}$ . The time of complete solidification, the temperature of the substrate surface in the contact region (see Fig. 1), and the crystallization rate (Fig. 2) vary insignificantly. A more intense heat transfer (a decrease in  $\delta_3$ ) from the droplet to the substrate leads to more intense supercooling (Fig. 1b) and to an increase in the temperature of the substrate surface in the contact spot (curve 1 in Fig. 3) and crystallization rate (curve 2 in Fig. 2). The crystallization time decreases thereby. As it follows from the calculations performed, there is practically no homogeneous nucleation because of the low supercooling. The crystalline phase appears and grows only on nanoparticles (seeds). The dispersion of the structure of the solidified melt is determined by the number of nanoparticles in the droplet volume. For the mass fraction of the modifying powder  $m_p = 5 \cdot 10^{-4}$  and  $R_p = 5 \cdot 10^{-8} \text{ m}$ , the number of particles (uniformly distributed) in a droplet of radius  $R_0 = 10^{-5} \text{ m}$  is  $N_p = 6450$ ; for  $R_p = 2.5 \cdot 10^{-8} \text{ m}$  and the same value of  $R_0$ , the number of particles is  $N_p = 51,600$ . It should be noted that crystallization for the cooling conditions considered starts after complete spreading of the droplet; the contact-spot radius  $R_c^s$  (and hence, the splat radius) is determined by the Reynolds number only and has the value of  $\sim 5.8 \cdot 10^{-5} \text{ m}$  (or  $R_c^s/R_0 = 5.8$ ) for  $v = 50 \text{ m/sec}$  and  $R_0 = 10^{-5} \text{ m}$ ; the height of the contact spot at the center ( $r = 0$ ) is  $H_0^s/R_0 = 0.238$ . These values are in reasonable agreement with the data summarized in [2]. A slightly higher value of  $R_c^s$  in the present work can be attributed to the fact that particle solidification during its spreading was taken into account in [2]. It

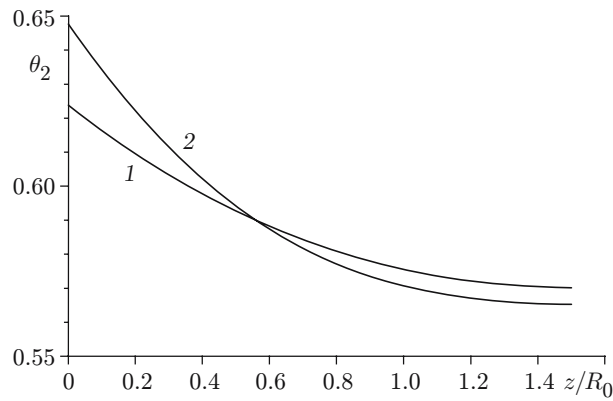


Fig. 4. Distribution of the substrate temperature along the  $z$  axis in the contact-spot region for  $\delta_3 = 10$  (curve 1) and  $5 \mu\text{m}$  (curve 2);  $R_p = 0.025\text{--}0.05 \mu\text{m}$ .

should also be noted that the numerical results support the validity of the assumptions made here, in particular, the neglect of the influence of the solid-phase fraction on the viscous properties of the melt and uniformity of the temperature field within the liquid layer, because the ratio of the time of passage of the heat wave for the spread particle  $t_T = (H_0^s)^2/a$  to the time of particle crystallization  $t_s \sim (1.0\text{--}1.6)R_0^2/a$  is much smaller than unity.

The influence of radiative heat transfer from the free surface on droplet cooling and crystallization was predicted to be negligibly small, i.e., the droplet is mainly cooled owing to heat transfer to the substrate. The behavior of the substrate temperature is illustrated in Fig. 4, which shows that the heating depth is approximately 1.5 droplet radii.

**Conclusions.** A model of nonequilibrium volume crystallization of a metallic droplet modified by activated refractory nanoparticles upon its impact onto a solid substrate is proposed. Conditions of applicability of this model are described, and specific features of the melt-crystallization kinetics depending on intensity of heat transfer to the substrate and concentration and characteristic size of modifying nanoparticles are examined. It is demonstrated that the dispersion of the crystalline structure of splats can be effectively controlled by adding small amounts of highly activated ultrafine seeds.

This work was supported by the Program of the Presidium of the Siberian Division of the Russian Academy of Sciences “Basic Problems in Physics and Chemistry of Nanoscale Systems and Nanomaterials” and by the Integration Project No. 93 of the Siberian Division of the Russian Academy of Sciences in 2003–2005.

## REFERENCES

1. V. V. Kudinov, *Plasma Coatings* [in Russian], Nauka, Moscow (1977).
2. O. P. Solonenko, A. P. Alkhimov, V. V. Marusin, et al., *High-Energy Processes in Material Processing*, Vol. 18: *Low-Temperature Plasma* [in Russian], Nauka, Novosibirsk (2000).
3. A. N. Cherepanov, V. A. Poluboyarov, O. P. Solonenko, et al., “Impact of mechanical activation and modification of initial powder with refractory nanoparticles on the properties of plasma-sprayed coatings,” in: P. Fauchais (ed.), *Progress in Plasma Processing of Materials 2003*, Begell House, Inc., New York (2003), pp. 507–514.
4. D. A. Gasin and B. A. Uryukov, “Dynamics of interaction of a liquid drop with a surface,” *Izv. Sib. Otd. Akad. Nauk SSSR, Ser. Tekh. Nauk*, , No. 16, Issue 3, 95–100 (1986).
5. G. F. Balandin, *Fundamentals of the Ingot-Formation Theory* [in Russian], Mashinostroenie, Moscow (1979).
6. M. Flemings, *Solidification Processing*, McGraw-Hill, New York (1974).
7. A. I. Fedorchenko, “Hydrodynamic and thermophysical features of the impingement of melt drops onto solid surfaces,” Author’s Abstract, Doct. Dissertation in Phys.-Math. Sci., Novosibirsk (2000).
8. V. P. Saburov, E. N. Eremin, A. N. Cherepanov, et al., *Modification of Steel and Alloys by Disperse Seeds* [in Russian], Izd. Omsk. Gos. Tekh. Univ., Omsk (2002).
9. V. E. Zinov’ev, *Thermophysical Properties of Metals at High Temperatures* [in Russian], Metallurgiya, Moscow (1989).